

Article

Using Long-Lived Thorium Isotopes to Quantify the Lithogenic Inputs to the Lakes in Qaidam Basin, China

Chenyang Cao ^{1,†}, Chi Chen ^{2,†}, Pu Zhang ^{1,2,*} , Jiahui Cui ², Xuezheng Pei ¹, Xiangzhong Li ^{3,*} , Tiane Cheng ⁴, Lihua Liang ¹ and R. Lawrence Edwards ⁵

¹ College of Urban and Environmental Sciences, Northwest University, Xi'an 710127, China; caochenyang@stumail.nwu.edu.cn (C.C.); peixuezheng@stumail.nwu.edu.cn (X.P.); lianglh@nwu.edu.cn (L.L.)

² Institute of Global Environmental Change, Xi'an Jiaotong University, Xi'an 710061, China; 3120322032@stu.xjtu.edu.cn (C.C.); 3120322031@stu.xjtu.edu.cn (J.C.)

³ Yunnan Key Laboratory of Earth System Science, Yunnan University, Kunming 650500, China

⁴ School of Foreign Languages, Northwest University, Xi'an 710127, China; cte201707@nwu.edu.cn

⁵ Department of Earth and Environmental Sciences, University of Minnesota, Minneapolis, MN 55455, USA; edwar001@umn.edu

* Correspondence: zhangpu357@xjtu.edu.cn (P.Z.); xzhli04@163.com (X.L.)

† These authors contributed equally to this work.

Abstract: In the last decade, the ²³²Th–²³⁰Th system has gained popularity as a tracer to quantify lithogenic sources of trace elements to the marine environment. Thorium (Th) isotopes were utilized to quantify the supply of lithogenic inputs to Keluke Lake and Tuosu Lake in Qaidam Basin, China. A total of 33 water samples were collected from Keluke Lake, Tuosu Lake, and Bayin River to measure the concentrations of dissolved ²³²Th and ²³⁰Th. The relationship of ²³²Th concentration in the water was in the order Bayin River > Keluke Lake > KLK–TS River > Tuosu Lake, confirming the input of variable lithogenic material sources. Three sources dominate the flux of lithofacies into the lakes: the river input, the deposition of dust and the local input from the sediments surrounding the lakes. On an interannual timescale, the lithogenic flux of Keluke Lake was mainly derived from river input. In summer, the dust flux in the study area could be estimated as 0.133 g/m²/year, while the flux of lithogenic material from Bayin River to Keluke Lake was 12.367 g/m²/year. In contrast, the fluvial input to the Tuosu lake was small in comparison to the dust contribution of lithogenic flux. The high Th²³²-concentration and the vertical sediment flux in this lake may have been caused by resuspension of bottom sediments.

Keywords: the ²³²Th concentration; Qaidam Basin; lithogenic flux; dust flux; Keluke Lake; Tuosu Lake



Citation: Cao, C.; Chen, C.; Zhang, P.; Cui, J.; Pei, X.; Li, X.; Cheng, T.; Liang, L.; Edwards, R.L. Using Long-Lived Thorium Isotopes to Quantify the Lithogenic Inputs to the Lakes in Qaidam Basin, China. *Minerals* **2022**, *12*, 931. <https://doi.org/10.3390/min12080931>

Academic Editors: Alexander Malov and Oleg S. Pokrovsky

Received: 5 May 2022

Accepted: 21 July 2022

Published: 24 July 2022

Publisher's Note: MDPI stays neutral with regard to jurisdictional claims in published maps and institutional affiliations.



Copyright: © 2022 by the authors. Licensee MDPI, Basel, Switzerland. This article is an open access article distributed under the terms and conditions of the Creative Commons Attribution (CC BY) license (<https://creativecommons.org/licenses/by/4.0/>).

1. Introduction

The ocean is the ultimate receptor of continental erosion. On the surface of the ocean, this process occurs only through deposition of eolian mineral dust (also known as aerosol dust or simply dust) [1], and in some cases, dust is a major source of soluble micronutrients necessary for biological productivity [2]. Furthermore, it is also an external source of nutrients for marine and remote terrestrial ecosystems, due to the release of micronutrients such as iron, participating in carbon cycling processes [3–6]. Since the change in dust flux not only depends on regional climate change, but can also affect regional climate change, dust flux is one of the important factors in exploring regional climate environment [7]. In recent years, aerosol dust input to the ocean surface has been quantified using a combination of remote sensing and modelling techniques [8], but these models are still constrained by methods based on observational tracers, such as the use of dissolved Al [9] and dissolved Th [10]. Studying dust activity can help to better understand the links between various Earth environmental conditions, including climate, which are determined by the physical,

chemical, biological and human interactions that transform and transport matter and energy, which are the “Earth System”: a highly complex entity.

There are three natural radioactive decay systems in nature, namely, the uranium (U) system, thorium (Th) system and actinium–uranium (Ac-U) system, which start from ^{238}U , ^{232}Th and ^{235}U , respectively, and undergo multiple α and β decays to finally generate stable lead isotopes [11]. Important information on various processes taking place in the ocean can be provided by different isotopes of Th [12]. In marine systems, Th has been shown to be a helpful tracer, it has been applied to a wide range of oceanographic processes such as particle cycling [13–16], carbon export flux [17–19], boundary scavenging [20–23], and paleocirculation [24–26]. Under all redox conditions in natural waters, Th has only one stable oxidation state IV, with the highly particle-reactive [27], which makes Th easy to migrate from the water to particulate material, and as the particulate material settles, it is buried in the bottom sediments [28]. The sources of Th isotopes are very limited in the lake environment, among which the ^{232}Th isotope makes up approximately 99.98% of all natural Th isotopes, which are almost completely obtained by the dissolution of river, wind and lake sediments [29]. The disequilibrium of Th isotopes can be used to calculate rates and timescales of sinking particles, due to their unique and constant production rates from soluble parent nuclides of uranium and radium [27]. ^{230}Th is supplied to the ocean almost entirely by the decay of the highly soluble ^{234}U , which has a uniform distribution in the ocean [30]. ^{234}Th and ^{230}Th are derived from the alpha radioactive decay of ^{238}U and ^{234}U , and ^{228}Th is derived from the beta decay of ^{228}Ra in the ocean, respectively [10]. Since the inventory of uranium nuclides and their isotopic compositions were largely unchanged during the years in the saline, the production rates of ^{234}Th and ^{230}Th have remained essentially stable [31]. Due to the particle reactivity and constrained sources, Th isotopes are considered to be a useful tool to study particle fluxes and sedimentary record in the ocean [32]. ^{232}Th can act as a tracer of lithogenic input, while ^{230}Th provides information concerning residence time with respect to scavenging; thus, long-lived Th isotopes can be used to track and quantify the input of lithogenic material to the ocean [33]. ^{230}Th can be used to evaluate the scavenging rate of seawater [34], and some researchers have used ^{230}Th to trace particles and water masses to explore the circulation and ventilation process of the water in the Southern Ocean [35]. Hayes et al. [36] used long-lived thorium isotopes to quantify lithogenic input in the North Pacific, and the calculated dissolved Th fluxes can be used to estimate fluxes of dissolved metals from other diagenetic sources as well as fluxes of primary diagenetic supplies, such as aerosol dust deposits [36].

In the past decade, the ^{232}Th – ^{230}Th system has received more and more attention as a tracer system for quantifying the lithogenic sources of trace elements in the marine environment [10,36–39]. However, research on lithogenic sources of inland lakes, especially inland salt lakes/saltwater lakes under a high-altitude arid climate, is limited. The research area of this study was Qaidam Basin, on the northeastern edge of the Qinghai–Tibet Plateau, where there are many large salt lakes/saltwater lakes. The Qinghai–Tibet Plateau is one of the most sensitive regions to global climate change, with completely different regional climate characteristics [40]. According to a previous study on Qinghai Lake, Qinghai–Tibet Plateau, the lithogenic flux is highly related to atmospheric dust and the input of recharge rivers, and dust flux contributes the main source of lithogenic flux in the southeast lake, which is $\sim 0.109\text{ g/m}^2/\text{year}$, while the main source of flux in the northwest lake area is recharge water, accounting for about 90% of the lake detrital flux [40]. Since Qinghai Lake has five recharging rivers with obvious seasonal variations, it is to be further determined whether the debris enters the rivers and then the lake due to atmospheric wet deposition or riverbed erosion. Second, because of the complexity of external lithogenic sources entering the Qinghai Lake, which brings a large uncertainty for quantitative assessment of lithogenic flux, it is particularly important to choose a single source of recharge water and a single particle type for the river–lake system study.

In view of this, samples from Keluke Lake, Tuosu Lake, and Bayin River were selected for this study. The aims were to (1) estimate the ^{230}Th residence time of lake waters

by the ^{230}Th – ^{234}U disequilibrium, and (2) by investigating ^{232}Th content, try to quantify the ^{232}Th contributed by the river and atmospheric dust to the lakes, so as to explore the source of lithogenic flux in Keluke Lake and Tuosu Lake and understand its potential response to environmental change. The results provide basic information for understanding climate tracers and evaluating the distribution and flux sources of thorium in high-altitude lakes under the background of an arid environment. To some degree, the present study will contribute to the budget features of ^{230}Th and ^{232}Th as well as the corresponding geochemical significance in the lake area. Additionally, it also provides essential basic research data for exploring the paleo-oceanic processes of ^{230}Th in marine sediments.

2. Methodology

2.1. Study Sites

The study area ($37^{\circ}15'–37^{\circ}20'$ N, $96^{\circ}51'–96^{\circ}58'$ E) was located in Delingha city, Qinghai Province, northeast of Qaidam Basin. The Qaidam Basin, with an area of 120,000 km², is surrounded by the Kunlun Mountains to the south, the Altun Mountains to the west and the Qilian Mountains to the north and east. The surrounding mountains rise to an elevation of N5000 m above sea level, while the average elevation of the basin is 2800 m [41]. This region experiences a typical arid and semi-arid climate, with an average annual precipitation of 100 to 500 mm [42,43], much lower than the average annual evaporation of 1000 to 2000 mm [44–46]. Affected by the westerly climate and blocked by the high terrain, precipitation is rare and concentrated from May to September [47]. The mean annual temperature is about 4 °C around Tuosu Lake and Keluke Lake. The terrestrial vegetation is mainly desert vegetation, dominated by Chenopodiaceae, Ephedra, Nitraria, Compositae, *Glaux maritima* and *Triglochin maritimum* in Tuosu Lake and Keluke Lake catchments [48]. In Qaidam Basin, the main wind direction near the Keluke Lake is northeast. The sand-driving wind mainly occurs in winter and spring [49]. The wind energy environment is intermediate in Qaidam Basin. Annually, the sand activities are fiercest in the spring [50].

Bayin River ($36^{\circ}53'–38^{\circ}11'$ N, $96^{\circ}29'–98^{\circ}08'$ E), located in the northeast Qaidam Basin, is the largest river in Delingha and the fourth largest inland river in the basin. Bayin River originates in the south of Qilian Mountains [51] and is the main source of exogenous recharge water for Keluke Lake. Bayin River flows into Keluke Lake from the northeast and mixes with the original lake water, before flowing out of Keluke Lake from the southwest and eventually flowing into Tuosu Lake.

Freshwater Keluke Lake ($37^{\circ}14'–37^{\circ}20'$ N, $96^{\circ}51'–96^{\circ}57'$ E) is located in the NE Qaidam Basin on the NE Tibetan Plateau [52,53], covering an area of 57.9 km², with an average water depth of 2.9 m, salinity of 1.0 g/L, and pH of 8 [47,54]. Keluke Lake is in an arid desert climate with an average annual precipitation of 160 mm, and an average annual evaporation of 2000 mm (Delingha station, 30 km northeast of the lake) [52]. Keluke Lake is fed by two rivers from the surrounding mountains to the north and discharges through a small outlet stream (KLK-TS River) to terminal Tuosu Lake downstream. One of the inflowing rivers, Bayin River, is a large permanent river (with a mean discharge of 1.9×10^8 m³/year), while the smaller river to the west of the lake is now dry, due to the construction of an upstream dam [48,53]. The lake water has a mean residence time of 6 months, based on its total river inflow of 3.406×10^8 m³ and lake volume of 1.67×10^8 m³ [55]. Therefore, the reason Keluke Lake is freshwater in arid climates is that the main source of recharge is from snowmelt on the mountains that flow into the river.

Tuosu Lake ($37^{\circ}04'–37^{\circ}13'$ N, $96^{\circ}50'–97^{\circ}03'$ E) is a saltwater lake located 45 km southwest of Delingha city. The lake is connected to Keluke Lake, which is 3 km to the north, from which it is supplied through a connecting river. The shape of the lake is triangular, and there is a southeast–northwest lake island in the north of the lake center. The salinity of Tuosu Lake is 27.8 g/L, the pH value is 8.38, and the maximum depth is 23.6 m. As the estuary lake of Bayin River, the recharge water source of Tuosu Lake mainly comes from precipitation in the basin [56].

Keluke Lake is surrounded mostly by Quaternary lacustrine and alluvial deposits, and Tuosu Lake by Tertiary fine-grained deposits with limited groundwater storage capacity [52]. Keluke Lake is surrounded by dense marsh vegetation dominated by *Phragmites communis* along the littoral zone, while there is no marsh vegetation around Tuosu Lake [41].

2.2. Sampling Design and Methods

Water samples were collected from Tuosu Lake, Keluke Lake, Bayin River, and the river connecting Keluke Lake and Tuosu Lake (KLK–TS River) in four batches, from 2017 to 2021. A total of 28 water samples were collected from the surface and depth profiles of Tuosu Lake and Keluke Lake to investigate the spatial and vertical distribution differences in ^{232}Th concentrations in the lakes. The sample location distribution is shown in Figure 1.

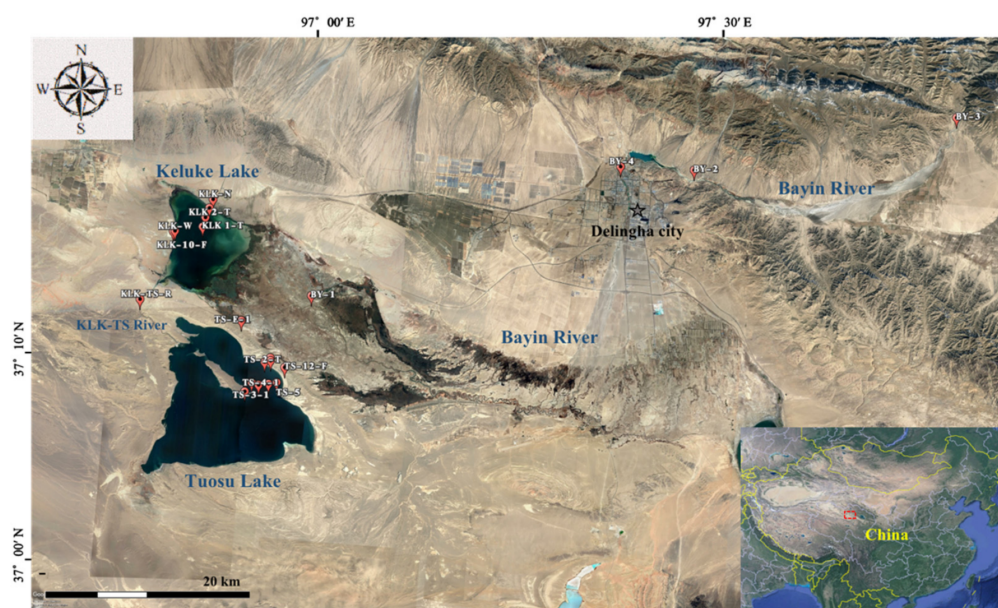


Figure 1. Study Sites in Qaidam Basin.

The first batch of sampling collected water samples from Tuosu Lake in December 2017. The second batch collected water samples from Tuosu Lake and Keluke Lake in June 2018. During the third sampling period, several surface water samples were collected from Tuosu Lake, Keluke Lake, Bayin River, and Keluke–Tuosu River in July 2019. In February 2021, two additional samples from Tuosu Lake and Keluke Lake were collected during the fourth sampling. In order to explore the effect of exogenous recharge river supply on the Th isotope concentration in the lake, five surface water samples were collected from the upper reaches (BY-3), middle reaches (BY-2), Delingha city (BY-4), and lower reaches (BY-1) of Bayin River and the river connecting Keluke Lake and Tuosu Lake.

Samples of surface water were collected in high-density polyethylene (HDPE) plastic bottles (Nalgene 2002-0032) while wearing Derma Free vinyl gloves. Other samples from different depths were collected using PMMA (polymethyl methacrylate) water traps and put into HDPE plastic bottles (Nalgene, 2002-0032). After collection, about 1000 mL of each sample was filtered through a mixed cellulose filter membrane (0.8 μm pore size, Millipore AAWP04700) with a manual vacuum filter system (Nalgene, 300-4100; Nalgene, 6133-0010), and the filtrate was stored for later analysis (Table 1).

Table 1. Sample information for water samples.

Location	Sample No.	Depth (m)	Latitude (°N) and Longitude (°E)	Date	Batch
Tuosu Lake	TS-1-1	0.5		9 December 2017	
	TS-1-2	10	37°08'40", 96°57'24"	9 December 2017	
	TS-1-3	21		9 December 2017	
	TS-2	4	37°09'11", 96°57'49"	9 December 2017	
	TS-3-1	0.2		9 December 2017	1
	TS-3-2	13	37°09'05", 96°58'18"	9 December 2017	
	TS-4-1	0.2		9 December 2017	
	TS-4-2	14	37°09'11", 96°58'58"	9 December 2017	
	TS-5	2	37°09'18", 96°59'31"	9 December 2017	
	TS-1-T	0.2		16 June 2018	
	TS-1-M	8	37°10'21", 96°58'35"	16 June 2018	
	TS-2-T	0.2		16 June 2018	
	TS-2-M	4.5	37°10'27", 96°58'59"	16 June 2018	2
	TS-3-T	0.2		16 June 2018	
	TS-3-M	3	37°10'36", 96°58'57"	16 June 2018	
	TS-E-1	0.2	37°12'29", 96°56'46"	22 July 2019	3
	TS-12-F	0.2	37°10'09", 96°59'59"	27 February 2021	4
	Keluke Lake	KLK 1-T	0.2		16 June 2018
KLK 1-M		2.5	37°17'24", 96°53'34"	16 June 2018	
KLK 1-B		4.5		16 June 2018	
KLK 2-T		0.2		16 June 2018	
KLK 2-M		1.5	37°17'55", 96°53'42"	16 June 2018	2
KLK 2-B		3.5		16 June 2018	
KLK 3-T		0.2		16 June 2018	
KLK 3-M		1	37°18'27", 96°53'55"	16 June 2018	
KLK-W		0.2	37°17'1", 96°51'35"	22 July 2019	
KLK-N		0.2	37°18'56", 96°54'7"	22 July 2019	3
KLK-10-F	0.2	37°17'03", 96°51'42"	27 February 2021	4	
Bayin River	BY-1	0.2	37°14'9", 97°1'23"	22 July 2019	
	BY-2	0.2	37°22'37", 97°26'44"	22 July 2019	
	BY-3	0.2	37°26'33", 97°44'19"	22 July 2019	3
	BY-4	0.2	37°22'30", 97°21'43"	22 July 2019	
KLK-TS River	KLK-TS-R	0.2	37°13'11", 96°49'44"	22 July 2019	3

2.3. Analytical Methods

The experimental analysis methods included two steps: chemical separation and MC-ICP-MS mass spectrometry. The former included sample digestion, centrifugal coprecipitation, ion exchange resin separation, collection as well as purification. To be specific, each sample was weighted and spiked with ^{233}U - ^{236}U - ^{229}Th , preconcentrated and digested with HNO_3 and HClO_4 . The sample was heated and dried, then dissolved with 2 N HCl. Then, 3–5 drops of Fe solution were added to the sample, and $\text{NH}_3 \cdot \text{H}_2\text{O}$ was used to adjust the pH of the sample to 8–9. The sample was mixed well and left for a while until a yellow precipitate appeared at the bottom of the bottle. The Fe precipitate was transferred to a centrifuge tube and centrifuged 2–3 times and then rinsed with deionized H_2O (>18 M Ω) to remove the water-soluble cation and avoid the influence of other metal ions and soluble impurities. The centrifuged precipitate was dissolved by 14 N HNO_3 and transferred to a Teflon beaker, before being heated and dried for subsequent treatment. The precipitate was completely dissolved using 7 N HNO_3 before being moved to a preprepared AG1-X8 anion-exchange resin column, and then 3 CVs of 7 N HNO_3 was added to remove Fe (CV: column volume) and 3 CVs of 6 N HCl to achieve the Th isotope separation process. The collected Th solution was dried by adding 2 drops of HClO_4 and dissolved in dilute acid (2% HNO_3 + 0.01% HF) for subsequent mass spectrometry analysis.

For instrument analysis, the Th isotopes were measured by the Thermo Fisher's Neptune Plus MC-ICP-MS. All measurements were conducted by following a peak-jumping

routine in ion counting mode on the discreet dynode multiplier behind the retarding potential quadrupole. The measurement of each sample was bracketed by measuring an aliquot of the run solution, which was used to adjust the instrument background count rates on the measured masses. The measurement uncertainties of Th included propagated errors from the ICP-MS isotope ratio measurements, spike concentrations, and blank corrections. The procedural blanks for chemical as well as mass spectrometric analyses at the Laboratory of Isotope Geochemistry in Xi'an Jiao Tong University were around 205 fg (5.3×10^6 atoms) for ^{232}Th and 37 ag (1.0×10^5 atoms) for ^{230}Th . The methods adopted herein were elaborated upon by Cheng et al. [57,58] and Shen et al. [59,60].

Due to the decay of ^{234}U during sample retention, the measured ^{230}Th concentrations must be corrected for in-growth. In order to utilize ^{230}Th – ^{234}U disequilibrium to obtain the Th residence time, the ^{230}Th s must also be corrected according to the proportion of ^{230}Th released by the dissolution of lithogenic substances. This adjustment is performed with concurrent measurements of ^{232}Th , with a lithogenic ratio of $^{230}\text{Th}/^{232}\text{Th} = 4.0 \times 10^{-6}$ mol/mol [61].

2.4. Theory

The particle-reactive isotopes in the U and Th decay series are useful tracers of particulate flux in water [62]. Long-lived thorium isotopes (half-life of $^{232}\text{Th} = 14.1 \times 10^9$ years; half-life of $^{230}\text{Th} = 75.6 \times 10^3$ years) provide a method for determining the cycling rates of lithogenic element in seawater [36,63]. The Th residence time can be calculated by the production rate of ^{230}Th in the water column under stable conditions. The flux of ^{232}Th can then be obtained by combining the residence time with the inventory of ^{230}Th , subsequently, the flux of terrestrial or atmospheric deposition can be extrapolated (e.g., the ^{230}Th normalization technique) [36,37,40]. Lastly, the input and flux of lithogenic particles and trace elements to the ocean can be estimated by the knowledge about the composition and solubility of the lithogenic material [10,64]. The scavenging rate of Th equals the inverse of its corresponding residence time (τ_{Th}). When assuming steady-state against production by uranium decay, τ_{Th} can be quantified by using measurements of dissolved ^{230}Th . The production of ^{230}Th is obtained by multiplying the activity of ^{234}U by the radioactive decay rate of ^{230}Th ($\lambda_{230} = 9.1705 \times 10^{-6}$) [58]. Inventories of both ^{230}Th and its production due to ^{234}U decay then can be used to calculate residence time as a function of integrated depth (Equation (1)) [36]:

$$\tau_{\text{Th}}(z) = \frac{\int_0^z \text{dissolved}^{230}\text{Thxs} dz}{\int_0^z \text{activity}^{234}\text{U} \times \lambda_{230} dz} \quad (1)$$

With knowledge of the Th residence time derived from ^{230}Th , the flux of dust-derived ^{232}Th necessary can be calculated to support the observed ^{232}Th inventory [38]. The dissolved ^{232}Th flux can be calculated by integrating the dissolved ^{232}Th from the surface to the integration depth and dividing by the corresponding ^{230}Th residence time (Equation (1)). The calculation formula of dissolved ^{232}Th flux in lake water is as Equation (2) [36].

$$\text{dissolved}^{232}\text{Th flux}(z) = \frac{\int_0^z \text{d}^{232}\text{Th} dz \times \int_0^z (\lambda_{230}^{234}\text{U}) dz}{\int_0^z \text{d}^{230}\text{Thxs} dz} = \frac{\int_0^z \text{d}^{232}\text{Th} dz}{\tau_{\text{Th}}} \quad (2)$$

The lithogenic material flux can then be estimated by dividing the dissolved ^{232}Th flux by the content of ^{232}Th in the basaltic lithogenic material around the Qinghai region ($[\text{Th}]_{\text{litho}}$) and the fractional solubility of ^{232}Th in lithogenic material (S_{Th}). According to a previous study, the basaltic lithogenic material around the Qinghai region is $10.5 \mu\text{g/g}$ [65]. The calculation formula is as Equation (3) [36]. Based on the preliminary results of lake particles in the Qaidam Basin, the ^{232}Th solubility in Tuosu Lake and Keluke Lake ranged from 5% to 10% (unpublished data).

$$\text{Lithogenic flux}(z) = \frac{\text{Dissolved}^{232}\text{Th flux}(z)}{[\text{Th}]_{\text{litho}} \times S_{\text{Th}}} \quad (3)$$

3. Results

3.1. Spatial Characteristics of Dissolved Th Isotope in the Lake Water

3.1.1. Surface Features of Dissolved Th Isotope in Surface Lake Water

The results of surface distribution features of dissolved Th isotope are obtained according to the water samples, 0.2 or 0.5 m below the lake surface, collected from seven sampling locations in Tuosu Lake and five sampling locations in Keluke Lake, which are presented in Table 2 and Figure 2.

Table 2. The dissolved ^{232}Th , dissolved ^{230}Th and dissolved $^{230}\text{Thxs}$ concentrations in Tuosu Lake, Keluke Lake and rivers.

Location	Sample No.	Depth	$d^{234}\text{U}$	$d^{232}\text{Th}$	$d^{230}\text{Th}$	$d^{230}\text{Thxs}$	Date
		(m)	(measured)	(pmol/kg)	($\mu\text{Bq/kg}$)	($\mu\text{Bq/kg}$)	
Tuosu Lake	TS-1-1	0.5	464.0	8.962	10.55	4.29	9 December 2017
	TS-3-1	0.2	463.2	0.640	11.97	11.52	9 December 2017
	TS-4-1	0.2	463.8	9.464	11.79	5.17	9 December 2017
	TS-1-T	0.2	461.9	0.042	-	-	16 June 2018
	TS-2-T	0.2	461.6	0.019	0.19	0.17	16 June 2018
	TS-3-T	0.2	460.3	0.045	-	-	16 June 2018
	TS-E-1	0.2	457.3	7.926	9.84	4.30	22 July 2019
	TS-1-2	10	462.1	9.942	12.00	5.06	9 December 2017
	TS-1-3	21	461.8	10.158	13.18	6.08	9 December 2017
	TS-2	4	462.2	8.437	12.77	6.87	9 December 2017
	TS-3-2	13	460.4	11.423	12.94	4.95	9 December 2017
	TS-4-2	14	460.4	11.710	14.53	6.34	9 December 2017
	TS-5	2	461.2	10.520	13.06	5.71	9 December 2017
	TS-1-M	8	462.0	0.045	-	-	16 June 2018
	TS-2-M	4.5	461.1	0.022	-	-	16 June 2018
TS-3-M	3	462.1	0.057	-	-	16 June 2018	
Keluke Lake	KLK 1-T	0.2	505.5	1.336	1.34	0.41	16 June 2018
	KLK 2-T	0.2	503.9	1.126	0.82	0.04	16 June 2018
	KLK 3-T	0.2	501.7	1.167	1.54	0.73	16 June 2018
	KLK-W	0.2	476.4	1.699	2.96	1.78	22 July 2019
	KLK-N	0.2	451.0	2.551	1.92	0.13	22 July 2019
	KLK 1-M	2.5	506.4	0.975	0.61	0.04	16 June 2018
	KLK 1-B	4.5	503.4	1.228	0.98	0.13	16 June 2018
	KLK 2-M	1.5	505.9	1.552	1.18	0.09	16 June 2018
	KLK 2-B	3.5	503.6	0.442	1.11	0.80	16 June 2018
KLK 3-M	1	504.0	0.864	0.68	0.07	16 June 2018	
Bayin River	BY-1	0.2	464.4	4.771	4.43	1.09	22 July 2019
	BY-2	0.2	401.9	1.583	0.86	0.31	22 July 2019
	BY-3	0.2	392.1	3.181	1.60	0.49	22 July 2019
	BY-4	0.2	408.8	0.599	0.02	-	22 July 2019
KLK-TS River	KLK-TS-R	0.2	482.1	1.078	0.88	0.13	22 July 2019

Note: “-” means invalid data.

In Tuosu Lake, the ^{232}Th showed significant uneven concentration distribution cross the surface lake, ranging from 0.019 to 9.464 pmol/kg and averaging 3.871 pmol/kg; the maximum value occurred at TS-4-1, and the minimum value occurred at TS-2-T. The details are shown in Figure 2. The total dissolved ^{230}Th concentration ranged from 0.19 to 11.97 $\mu\text{Bq/kg}$, with an average of 8.87 $\mu\text{Bq/kg}$; the maximum value occurred at TS-3-1, while the minimum occurred at TS-2-T. The $^{230}\text{Thxs}$ content of Tuosu Lake ranged from 0.17 to 11.52 $\mu\text{Bq/kg}$ with a mean value of 5.09 $\mu\text{Bq/kg}$.

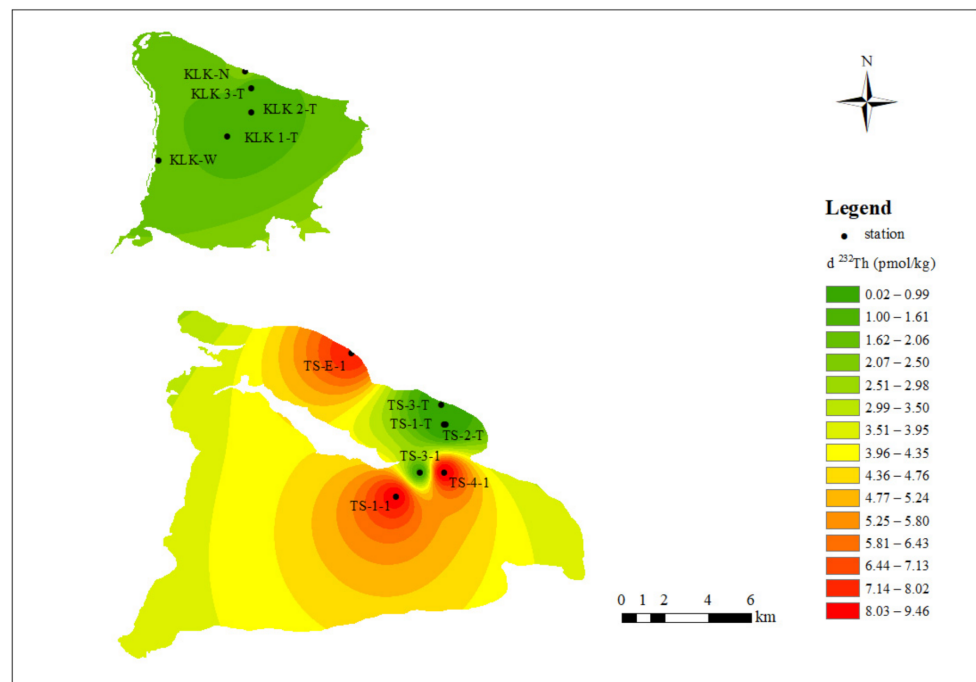


Figure 2. Surface distribution features of dissolved ^{232}Th concentration in Tuosu Lake and Keluke Lake.

In Keluke Lake, the ^{232}Th concentration varied from 1.126 to 2.551 pmol/kg, averaging 1.576 pmol/kg. The total dissolved ^{230}Th concentration ranged from 0.82 to 2.96 $\mu\text{Bq}/\text{kg}$, whose mean value was 1.72 $\mu\text{Bq}/\text{kg}$. The $^{230}\text{Th}_{\text{xs}}$ concentration ranged from 0.04 to 1.78 $\mu\text{Bq}/\text{kg}$, with a mean value of 0.62 $\mu\text{Bq}/\text{kg}$.

In conclusion, significant differences were found in the concentrations of ^{232}Th , ^{230}Th , and $^{230}\text{Th}_{\text{xs}}$ in the surface water of Tuosu Lake, but limited variation in Keluke Lake. The concentration of ^{232}Th at TS-1-1 and TS-4-1, located in the central area of Tuosu Lake, was significantly higher than at the edge of the east area of the lake. At the same time, the concentrations of ^{230}Th and $^{230}\text{Th}_{\text{xs}}$ in the central area of Tuosu Lake were much higher than at the eastern edge of the lake. As for Keluke Lake, the concentrations of ^{232}Th , ^{230}Th , and $^{230}\text{Th}_{\text{xs}}$ in the surface water were basically uniform, with limited variation.

3.1.2. Distribution Features of Dissolved Th Isotope in Depth Profiles of Lake Water

Samples were collected at varying depths at eight sites in Tuosu Lake and three sites in Keluke Lake, and the results are shown in Table 2. From the surface to the bottom of Tuosu Lake, the ^{232}Th concentration of each depth profile exhibited a gradual increase with depth and reached its maximum at the bottom of the lake. Notably, the ^{232}Th concentration at depth profile sites located far from the lakeshore was much higher than at the eastern edge of the lakeshore, which ranged from 0.640 to 11.423 pmol/kg, and had a mean value of 9.028 pmol/kg. The ^{232}Th concentration of depth profile sites located at the eastern edge of the lake ranged from 0.019 to 0.057 pmol/kg, averaging 0.038 pmol/kg. Like the concentration of ^{232}Th , the total dissolved ^{230}Th concentration increased with depth, reaching its maximum at the bottom of the lake. In the central area of Tuosu Lake, the total dissolved ^{230}Th concentration varied from 10.55 to 13.18 $\mu\text{Bq}/\text{kg}$, averaging 12.53 $\mu\text{Bq}/\text{kg}$, while in the marginal area, it was 0.19 $\mu\text{Bq}/\text{kg}$. The $^{230}\text{Th}_{\text{xs}}$ content of the center lake ranged from 4.29 to 11.52 $\mu\text{Bq}/\text{kg}$, with an average of 6.22 $\mu\text{Bq}/\text{kg}$, while that at the edge area of the lake was 0.17 $\mu\text{Bq}/\text{kg}$.

In Keluke Lake, the results of the three depth profiles showed that the variation of ^{232}Th concentration was limited with depth, basically showing a decreasing trend with increasing depth. There was little variation across the different depth profile sites, ranging from 0.442 to 1.552 pmol/kg and averaging 1.086 pmol/kg. The total dissolved ^{230}Th

concentration in Keluke Lake ranged from 0.61 to 1.54 $\mu\text{Bq/kg}$, averaging 1.03 $\mu\text{Bq/kg}$. The concentration of $^{230}\text{Thxs}$ ranged from 0.04 to 0.80 $\mu\text{Bq/kg}$, averaging 0.29 $\mu\text{Bq/kg}$. The total dissolved ^{230}Th concentration and $^{230}\text{Thxs}$ concentration at both KLK-1 and KLK-3 depth profile sites decreased with depth, whereas the opposite was true at the KLK-2 site. The details are shown in Figure 3.

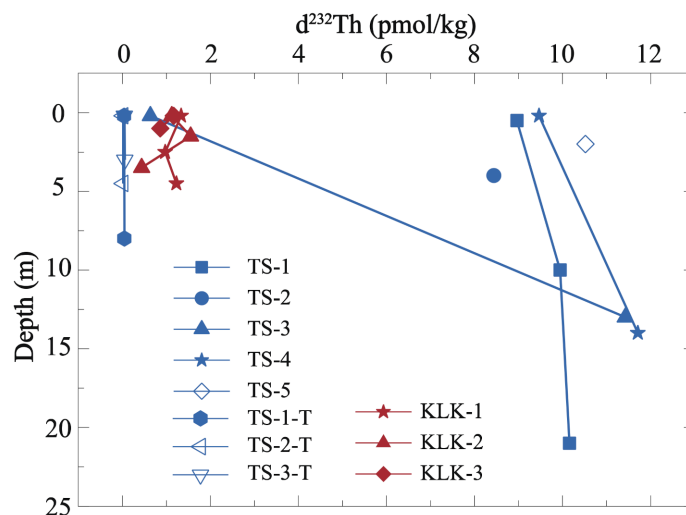


Figure 3. Distribution features of dissolved ^{232}Th concentration in the depth profiles of Tuosu Lake and Keluke Lake.

3.2. Seasonal Distribution Characteristics of Dissolved Th Isotope in Lake Water

Due to the dissolved Th isotope exhibiting seasonal differences in lake water, seven samples in different months from Tuosu Lake and Keluke Lake were selected for analysis and comparison. There were visible seasonal variations in the ^{232}Th content, total dissolved ^{230}Th concentration, and $^{230}\text{Thxs}$ concentration in the lakes. The details are shown in Table 3. In both Tuosu Lake and Keluke Lake, the samples from December and February had higher Th isotope concentrations than that from June and July. The concentration of ^{232}Th in samples from February was tens to hundreds of times greater than that in other months in Tuosu Lake, while the concentration in samples from February was tens of times greater than that from June and July in Keluke Lake.

Table 3. Seasonal changes in dissolved Th isotope in Tuosu Lake and Keluke Lake.

Location	Sample No.	Depth (m)	$d^{234}\text{U}$ (measured)	$d^{232}\text{Th}$ (pmol/kg)	$d^{230}\text{Th}$ ($\mu\text{Bq/kg}$)	$d^{230}\text{Thxs}$ ($\mu\text{Bq/kg}$)	Latitude ($^{\circ}\text{N}$) and Longitude ($^{\circ}\text{E}$)	Date
Tuosu Lake	TS-4-1	0.2	463.8	9.464	11.79	5.17	$37^{\circ}09'11''$, $96^{\circ}58'58''$	9 December 2017
	TS-2-T	0.2	461.6	0.019	0.19	0.17	$37^{\circ}10'27''$, $96^{\circ}58'59''$	16 June 2018
	TS-E-1	0.2	457.3	7.926	9.84	4.30	$37^{\circ}12'29''$, $96^{\circ}56'46''$	22 July 2019
	TS-12-F	0.2	472.2	86.286	69.07	8.77	$37^{\circ}10'09''$, $96^{\circ}59'59''$	27 February 2021
Keluke Lake	KLK 1-T	0.2	505.5	1.336	1.34	0.41	$37^{\circ}17'24''$, $96^{\circ}53'34''$	16 June 2018
	KLK-W	0.2	476.4	1.699	2.96	1.78	$37^{\circ}17'1''$, $96^{\circ}51'35''$	22 July 2019
	KLK-10-F	0.2	504.3	18.432	13.59	0.71	$37^{\circ}17'03''$, $96^{\circ}51'42''$	27 February 2021

3.3. Features of Dissolved Th Isotope Concentration Distribution in Exogenous Recharged River Waters

In Bayin River, the concentration of ^{232}Th ranged from 0.599 to 4.771 pmol/kg, averaging 2.534 pmol/kg, which is higher than that in Keluke Lake but lower than that in Tuosu Lake (Table 3). The total dissolved ^{230}Th concentration of Bayin River ranged from 0.02 to 4.43 $\mu\text{Bq/kg}$, whose mean value was 1.73 $\mu\text{Bq/kg}$. The concentration of $^{230}\text{Thxs}$ ranged from 0.31 to 1.09 $\mu\text{Bq/kg}$ with a mean value of 0.63 $\mu\text{Bq/kg}$. The total dissolved ^{230}Th concentration and $^{230}\text{Thxs}$ concentration of Bayin River were close to that of Keluke Lake.

In the river connecting Keluke Lake and Tuosu Lake (KLK–TS River), the concentration of ²³²Th was 1.078 pmol/kg, lower than the mean concentration in Bayin River, which was between the ²³²Th concentrations in Tuosu Lake and Keluke Lake. The total dissolved ²³⁰Th and ²³⁰Thxs concentrations were 0.88 μBq/kg and 0.13 μBq/kg, respectively, the lowest among all site averages.

4. Discussion

4.1. Th Scavenging Residence Time in Lake Water

4.1.1. Th Scavenging Residence Time in Surface Lake Water

According to Equation (1), we determined the ²³⁰Th increment generated from ²³⁴U decay in the surface water in Tuosu Lake and Keluke Lake and obtained the ²³⁰Th residence time (τTh) in the water columns of both lakes.

As shown in Table 4, in Tuosu Lake, the ²³⁰Th scavenging residence time of surface water samples collected in December ranged from 2.80 to 7.54 years, with a mean value of 4.57 years, while that of samples collected in June and July ranged from 0.11 to 2.85 years, with a mean value of 1.48 years. In Keluke Lake, the variation of the ²³⁰Th residence time in surface water samples was limited, ranging from 0.02 to 1.13 years, averaging 0.38 years, which is much lower than Tuosu Lake. The details are shown in Table 4. KLK-W, located at the western edge of Keluke Lake, had a significantly higher residence time than other sites, indicating a slower particle-scavenging rate.

Table 4. The dissolved ²³²Th concentration, τTh, dissolved ²³²Th flux, and lithogenic flux in Tuosu Lake and Keluke Lake.

Location	Sample No.	Depth	Density	d ²³² Th	τTh	d ²³² Th flux	Th-litho.flux S _{Th} = 5%	Th-litho.flux S _{Th} = 10%	Date
		(m)	(kg/m ³)	(pmol/kg)	(years)	(nmol/m ² /yr)	(g/m ² /yr)	(g/m ² /yr)	
Tuosu Lake	TS-1-1	0.5		8.962	2.80	1.634	0.722	0.361	9 December 2017
	TS-3-1	0.2		0.640	7.54	0.017	0.008	0.004	9 December 2017
	TS-4-1	0.2		9.464	3.38	0.572	0.253	0.126	9 December 2017
	TS-1-T	0.2	1021	0.042	-	-	-	-	16 June 2018
	TS-2-T	0.2		0.019	0.11	0.034	0.015	0.008	16 June 2018
	TS-3-T	0.2		0.045	-	-	-	-	16 June 2018
	TS-E-1	0.2		7.926	2.85	0.568	0.251	0.125	22 July 2019
	TS-1-2	10		9.942	3.31	30.632	13.536	6.768	9 December 2017
	TS-1-3	21		10.158	3.99	54.571	24.115	12.057	9 December 2017
	TS-2	4		8.437	4.50	7.650	3.380	1.690	9 December 2017
	TS-3-2	13		11.423	3.26	46.512	20.554	10.277	9 December 2017
	TS-4-2	14	1021	11.710	4.17	40.119	17.729	8.864	9 December 2017
	TS-5	2		10.520	3.75	5.727	2.531	1.265	9 December 2017
	TS-1-M	8		0.045	-	-	-	-	16 June 2018
TS-2-M	4.5		0.022	-	-	-	-	16 June 2018	
TS-3-M	3		0.057	-	-	-	-	16 June 2018	
Keluke Lake	KLK 1-T	0.2		1.336	0.24	1.099	0.486	0.243	16 June 2018
	KLK 2-T	0.2		1.126	0.02	10.695	4.726	2.363	16 June 2018
	KLK 3-T	0.2	1000	1.167	0.44	0.532	0.235	0.117	16 June 2018
	KLK-W	0.2		1.699	1.13	0.301	0.133	0.066	22 July 2019
	KLK-N	0.2		2.551	0.09	5.747	2.539	1.270	22 July 2019
	KLK 1-M	2.5		0.975	0.03	92.787	41.003	20.501	16 June 2018
	KLK 1-B	4.5		1.228	0.08	73.243	32.366	16.183	16 June 2018
	KLK 2-M	1.5	1000	1.552	0.06	41.303	18.252	9.126	16 June 2018
	KLK 2-B	3.5		0.442	0.48	3.218	1.422	0.711	16 June 2018
KLK 3-M	1		0.864	0.05	19.158	8.466	4.233	16 June 2018	

Note: The unit of the ²³²Th residence time obtained in Equation (1) is day. This table converts the unit to year for the convenience of discussion.

In summary, there were significant seasonal and spatial differences in the residence time of surface water in Tuosu Lake, indicating that the scavenging rate was inhomogeneous throughout the lake, related to the input of Keluke Lake and the subaerial erosion of an island in Tuosu Lake. The mean residence time of Tuosu Lake was larger than that of

Keluke Lake; therefore, Keluke Lake had more exogenous detrital material and a faster scavenging rate.

4.1.2. Th Scavenging Residence Time in Depth Profiles of Lake Water

In areas far from the edge of Tuosu Lake, the ^{230}Th data showed that the residence time of Th in the lake water at different depths ranged from 2.80 to 7.54 years, with a mean value of 4.08 years and little variation in the vertical profile (Table 4 and Figure 4). The short ^{230}Th residence time of TS-2-T indicates that it could be transferred more rapidly from the water column to sinking particulate matter through vertical fluxes, resulting in the scavenging rate being fast in the eastern edge area of Tuosu Lake. The variable disequilibrium between the different regions of the lake indicates more exogenous inputs at the edge of Tuosu Lake than away from the lake shore, which is highly consistent with the results observed in Qinghai Lake, another plateau salt lake [40]. It is worthy of note that the samples far from the edge of the lake were collected in winter, while the samples in the center of the lake were collected in summer; hence, there may have been seasonal differences in the scavenging rate of the water column.

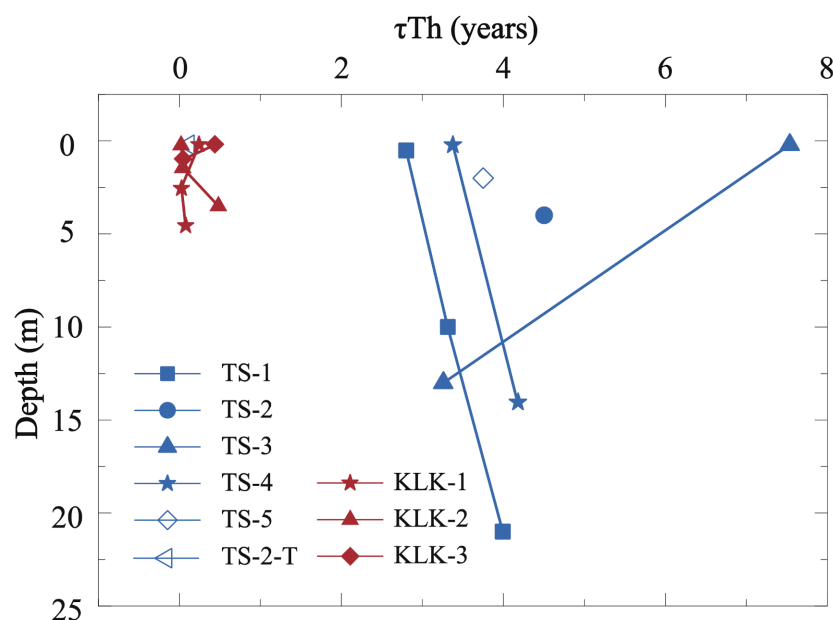


Figure 4. Distribution features of ^{230}Th residence time (τ_{Th}) in depth profiles of Tuosu Lake and Keluke Lake.

In Keluke Lake, the variation of the ^{230}Th residence time across the depth profiles was limited, ranging from 0.02 to 0.48 years, averaging 0.17 years, indicating slight difference in the scavenging rate of Th between different depths in the same area (Table 4 and Figure 4). The findings suggest a larger particulate matter size with faster removal rates according to ~ 0.5 years of deposition recorded in Keluke Lake. This indicates that Bayin River had more particle matter flux and/or larger particle size, mixing into the Keluke Lake with a hydraulic sorting effect.

In the same sampling season, the concentration of ^{232}Th in Keluke Lake was several hundred times higher than that in Tuosu Lake, but the difference in residence time was limited, indicating fewer exogenous particulate materials input to Tuosu Lake than to Keluke Lake. The differences in the depth profiles of Keluke Lake and Tuosu Lake may depend on variations in the river inflow, particle flux, and/or particle composition in different lakes. As a closed saltwater lake, the residence time of Tuosu Lake in December is 2–7 years, which is mainly affected by the sinking of particulate material. However, as an open freshwater lake, the residence time of Keluke Lake in June is less than 1 year, which is mainly affected by the mixing of young water from the recharge river with the lake.

4.2. Thorium-Derived Dissolved ^{232}Th Flux and Lithogenic Flux to Tuosu Lake and Keluke Lake

Previous studies confirmed that ^{232}Th concentrations of surface-water seem to be connected with the water column scavenging rate [63,66,67]. Thorium-232 ($t_{1/2} = 1.41 \times 10^{10}$ years) is nonradiogenic; thus, the source of ^{232}Th in water is mainly fluvial or aeolian detrital particulate material at the surface and continental margins [68]. More than 99.8% of Th in seawater is ^{232}Th , which is a primordial isotope, added to seawater in the dissolved pool through the partial dissolution of lithogenic materials [27]. Th is highly insoluble in water and is rapidly eliminated from solution by scavenging [69]. Therefore, without the influence of other factors, the ^{232}Th concentrations in water should decrease with depth and exhibit the maximum values in surface water [40]. Typical oceanic profiles of ^{232}Th correspondingly exhibit surface maxima and decreasing concentrations with depth [63].

According to previous studies [37,63,67], since most of the dissolved ^{232}Th in seawater originates from atmospheric dust which settles on the sea surface and dissolves into the ocean, the concentration of ^{232}Th in seawater decreases with depth and reaches the highest at the sea surface. Nevertheless, the opposite trend of ^{232}Th concentration was observed in Qinghai Lake on the Tibetan Plateau, China. Zhang et al. [40] suggested that the concentrations of ^{232}Th in the three depth profiles of Qinghai Lake were all positively correlated with depth, and the higher ^{232}Th values in the surface water might be related to the input of exogenous recharge rivers. Therefore, the sources of ^{232}Th in the lake are considered to be the dissolution of dust aerosols and inflow from the recharging rivers [31].

In Keluke Lake, the mean residence time is less than 1 year. The scavenging rate of lake water is fast, there is no long-term water–rock interaction, and groundwater contributes little to the recharge of the lake, the main source of recharge is from snowmelt on the mountains that flow into the river. Thus, even during freezing periods, the turn-over of the lake has limited effects on the residence time and the vertical transport of the lake water. Keluke Lake is surrounded by dense marsh vegetation dominated by *Phragmites communis* along the littoral zone, while there is no marsh vegetation around Tuosu Lake [33]. The biological activity in the two lakes is different, resulting in different sediment types. Keluke Lake is surrounded mostly by Quaternary lacustrine and alluvial deposits, and Tuosu Lake by Tertiary fine-grained deposits with limited groundwater storage capacity [52]. We compared the concentration of thorium in suspended particles and water in the two lakes (Table 5), and analyzed the rare earth elements (REE) in suspended particles (Figure 5). The REE data of suspended particles in Keluke Lake and Tuosu Lake indicate that the provenance of Th in the two lakes is consistent. The results show that Th in water is mainly affected by suspended particles, and the effect of biological activity is negligible. Therefore, Th in lake water can be an indicator of dust flux despite different biological activities in the two lakes.

Table 5. The concentration of thorium in suspended particles and water in Keluke Lake and Tuosu Lake.

Sample	Particle		Water	
	$^{232}\text{Th}(\text{pg/g})$	$^{230}\text{Th}(\text{fg/g})$	$^{232}\text{Th}(\text{pg/g})$	$^{230}\text{Th}(\text{ag/g})$
KLK-1-2-T	5.312	0.026	0.310	2.120
KLK-3-2-M	5.607	0.027	0.200	1.242
TS-1-2-T	7.058	0.033	9.693	0.349
TS-3-2	8.411	0.037	11.835	0.290

Furthermore, it takes time for particles to fall from the surface to the bottom of the lake, and time for thorium to transfer from atmospheric dust to the lake. Thus, Th isotopes in lake water can reflect the information of annual average dust flux, while Th in dust samples may only reflect instantaneous flux. Therefore, the lithogenic flux in the surface water can be used to estimate the contribution of atmospheric deposition to the particulate matter in the lake, and the depth profiles can be used to estimate the proportion of detrital particles contributed to the lake from the deep source.

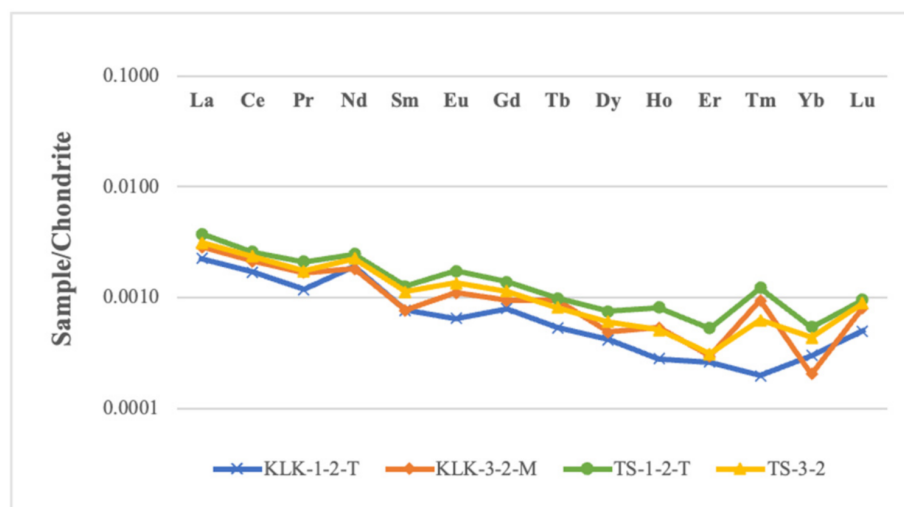


Figure 5. Chondrite-normalized REE patterns for different particles from Keluke Lake and Tuosu Lake.

4.2.1. The Spatial Trends of Dissolved ^{232}Th Flux and Lithogenic Flux in Lake Water

Within the study area, there was little variation in climatic characteristics. Therefore, in the case of ignoring other exogenous factors, the ^{232}Th contribution of atmospheric deposition to the lake surface water should be constant. However, the ^{232}Th concentration in the surface water of both Tuosu Lake and Keluke Lake showed an obvious uneven distribution (Figure 2). As for Keluke Lake, the average concentration of ^{232}Th (1.210 pmol/kg) was significantly higher than that of Tuosu Lake (0.035 pmol/kg) in June. Among all study areas, during the same sampling season, Bayin River had the highest concentration of ^{232}Th , followed by Keluke Lake, KLK–TS River, and Tuosu Lake, which had the lowest concentration of ^{232}Th . Therefore, it is reasonable to speculate that the detrital material carried by Bayin River was first input into Keluke Lake, before contributing additional ^{232}Th to Tuosu Lake via the KLK–TS River.

For Keluke Lake (Table 4 and Figure 6), the dissolved ^{232}Th flux in the surface water (mean value of 3.675 nmol/m²/year) is much higher than that in Tuosu Lake (mean value of 0.565 nmol/m²/year). When the Th solubility from particles is 5%, the fluxes of lithogenic material in the surface water ranged from 0.008 to 0.722 g/m²/year in Tuosu Lake, and from 0.133 to 4.726 g/m²/year in Keluke Lake (Table 4 and Figure 7). The lithogenic flux in Keluke Lake was several to tens of times higher than that in Tuosu Lake. The differences in dissolved ^{232}Th flux and lithogenic flux between these two lakes indicate that, in addition to atmospheric dust, Keluke Lake had more exogenous detrital material from the recharging river, which substantially contributed ^{232}Th to Keluke Lake, leading to the characteristic of high flux. However, the contribution of exogenous ^{232}Th from Bayin River to Tuosu Lake was limited. Therefore, in the same sampling season (June and July), when the influence of exogenous supply on Tuosu Lake was ignored, the dust flux in the study area could be calculated using the surface water data of Tuosu Lake, which was 0.133 g/m²/year, accounting for 8% of the total flux contribution to Keluke lake.

4.2.2. The Depth Trends of Dissolved ^{232}Th Flux and Lithogenic Flux in Lake Water

The input of the exogenous recharge river may have affected the variation of ^{232}Th flux and lithogenic flux in the water columns of Tuosu Lake and Keluke Lake, ultimately affecting the vertical distribution features of ^{232}Th concentration in the lakes. The dissolved ^{232}Th flux and lithogenic flux of the vertical gradient in the lakes was calculated using Equations (2) and (3). The details are shown in Table 4.

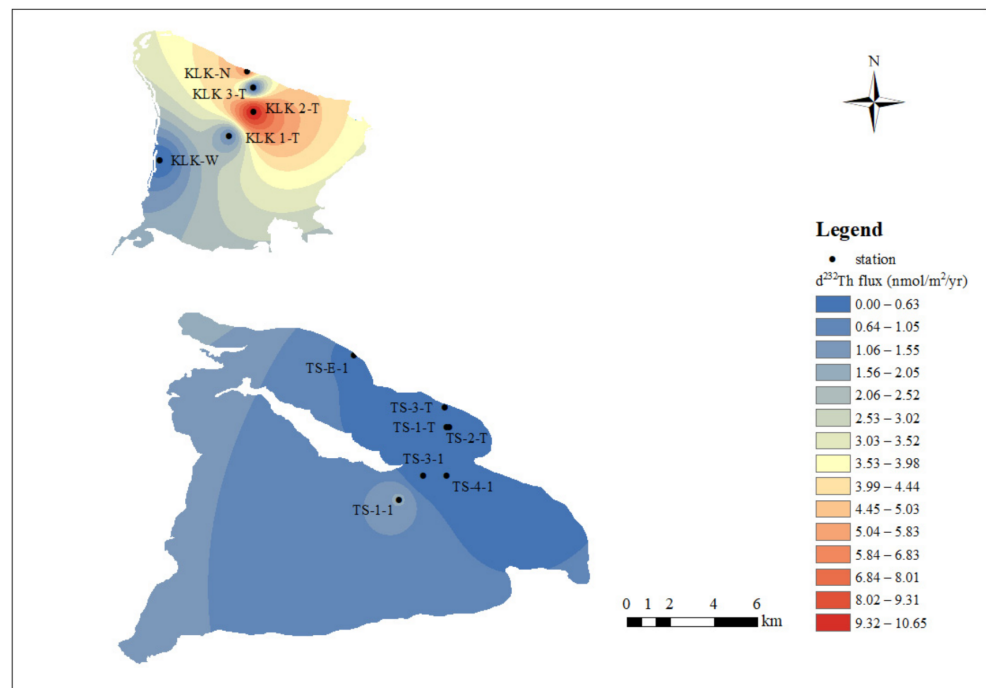


Figure 6. Distribution features of dissolved ²³²Th flux in the surface water of Tuosu Lake and Keluke Lake.

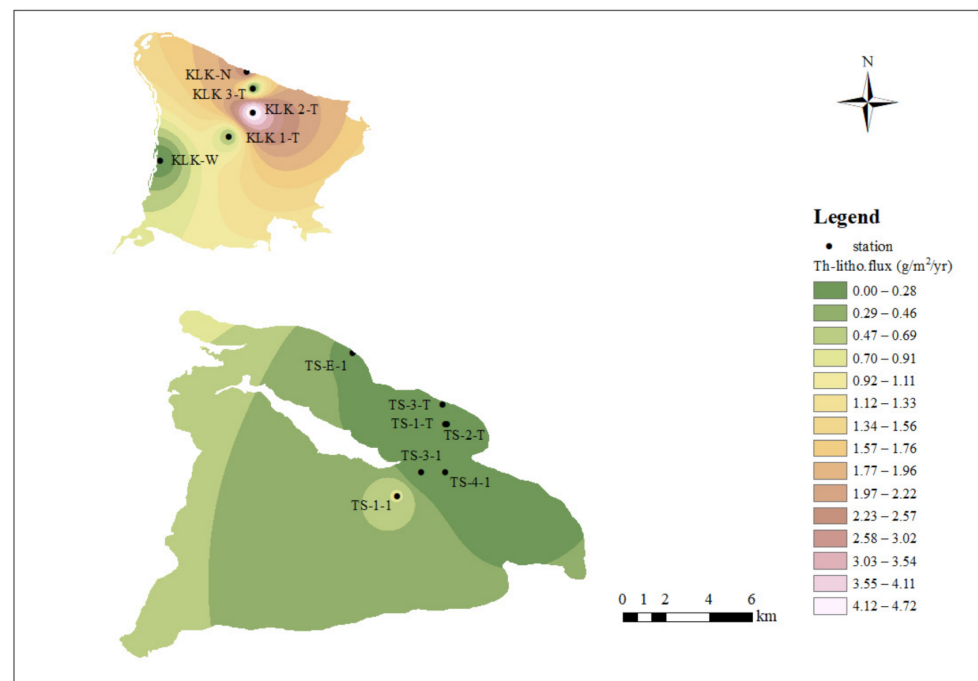


Figure 7. Distribution features of lithogenic flux in the surface water of Tuosu Lake and Keluke Lake.

In Tuosu Lake, dissolved ²³²Th flux and lithogenic flux in all depth profiles exhibited an increasing trend with depth (Table 4 and Figure 8). There was little difference between the mean values of fluxes in different depth profiles. The eastern edge of Tuosu Lake had slightly lower fluxes than the central island area of the lake, showing a great relationship with the contribution of continental material to the water column by the island in the middle of Tuosu Lake. In Keluke Lake, dissolved ²³²Th flux and lithogenic flux increased with depth from the surface and then decreased at the bottom of the lake (Table 4 and Figure 8), which is consistent with the fluxes observed in Qinghai Lake [40].

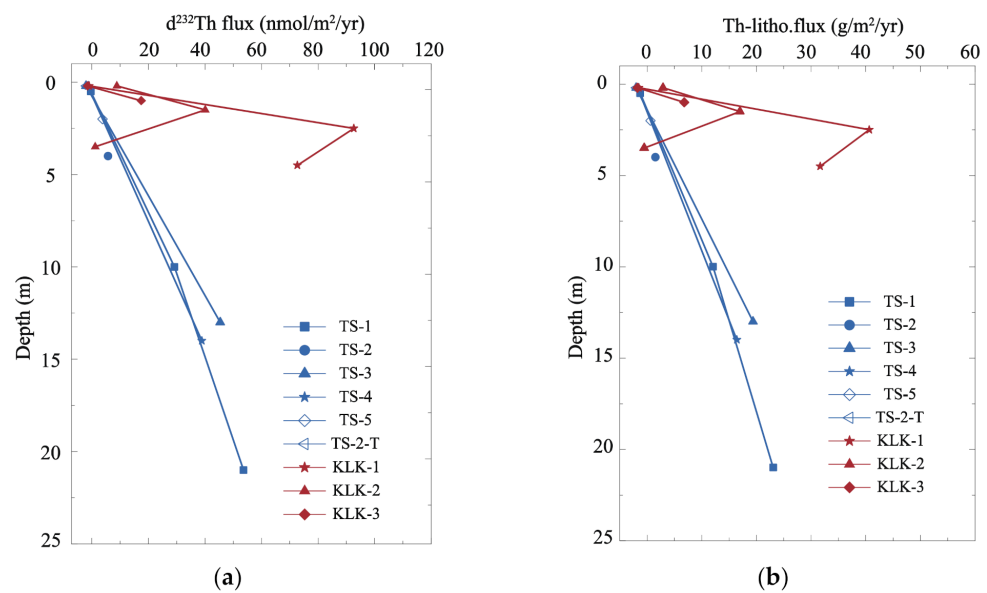


Figure 8. Distribution features of dissolved ^{232}Th flux (a) and lithogenic flux (b) in the depth profiles of Tuosu Lake and Keluke Lake.

The average ^{232}Th flux and lithogenic flux of Keluke Lake were several times that of Tuosu Lake, and the variation range of fluxes was much higher. The water flux values of Keluke Lake at the middle depth were the highest, indicating that the exogenous recharge river carried a large number of detrital particles, contributing most of the ^{232}Th to the lake. These particulate materials mixed with Keluke Lake water and then flowed into Tuosu Lake via KLK–TS River, contributing a small amount of ^{232}Th to Tuosu Lake.

4.2.3. Seasonal Changes in Dissolved ^{232}Th Flux and Lithogenic Flux in Lake Water

In view of the significant seasonal variation of dissolved ^{232}Th isotope in lake water, seven samples from Tuosu Lake and Keluke Lake were selected in different months to analyze the seasonal variation of their fluxes. The details are shown in Table 6. In both Tuosu Lake and Keluke Lake, dissolved ^{232}Th flux and lithogenic flux were at least several times higher in winter than in summer, reaching their maximum values in February, consistent with their dissolved Th isotope concentrations. The research of Zhang et al. [40] showed that in the dry season, with little precipitation October through May, the content of ^{232}Th in rivers in Qinghai region from June to September is higher than that in the rainy season. Therefore, the recharge rivers contributed more exogenous material to the lakes in winter than in summer, resulting in significant seasonal changes in flux values for both lakes. In addition, even if the lake is covered with ice in winter, thorium enters the water as the ice melts. Therefore, we believe that although there are obvious seasonal differences in thorium in lake water, thorium in the water column of samples collected in summer can reflect the annual average dust flux.

In Qaidam Basin, the main wind direction near the study area is northeast. The sand-driving wind mainly occurs in winter and spring [49]. The wind energy environment is intermediate in Qaidam Basin. Annually, the sand activities are fiercest in the spring [50]. Topographically, Keluke Lake is surrounded by flat wetlands, while Tuosu Lake is surrounded by hills. In view of this, during the windy winter and spring, the deposition of atmospheric dust contributed a large amount of lithogenic flux to the lakes, and the regional topography of the two lakes resulted in a 36% lower flux in Tuosu Lake than in Keluke Lake. By comparing the maximum surface water flux of Keluke Lake in winter and summer, it can be inferred that the lithogenic flux of the lake was mainly from river input, whereby the contribution of particulate material carried by Bayin River to lake flux was 19% higher than that of atmospheric dust on an interannual timescale.

Table 6. Seasonal changes in dissolved ^{232}Th flux and lithogenic flux in Tuosu Lake and Keluke Lake.

Location	Sample No.	Depth	Density	$d^{232}\text{Th}$	τTh	$d^{232}\text{Th}$ flux	Th-litho.flux $S_{\text{Th}} = 5\%$	Th-litho.flux $S_{\text{Th}} = 10\%$	Date
		(m)	(kg/m^3)	(pmol/kg)	(years)	($\text{nmol}/\text{m}^2/\text{yr}$)	($\text{g}/\text{m}^2/\text{yr}$)	($\text{g}/\text{m}^2/\text{yr}$)	
Tuosu Lake	TS-4-1	0.2		9.464	3.38	0.572	0.253	0.126	9 December 2017
	TS-2-T	0.2	1021	0.019	0.11	0.034	0.015	0.008	16 June 2018
	TS-E-1	0.2		7.926	2.85	0.568	0.251	0.125	22 July 2019
	TS-12-F	0.2		86.286	5.62	3.133	1.384	0.692	27 February 2021
Keluke Lake	KLK 1-T	0.2			1.336	0.24	1.099	0.486	0.243
	KLK-W	0.2	1000	1.699	1.13	0.301	0.133	0.066	22 July 2019
	KLK-10-F	0.2		18.432	0.42	8.690	3.840	1.920	27 February 2021

4.3. Contribution of Recharging River and Atmospheric Dust to ^{232}Th Fluxes in Lake Water Column

A past study confirmed that the ^{238}U concentration and the activity ratios of $^{234}\text{U}/^{238}\text{U}$ in Tuosu Lake and Keluke Lake showed a uniform distribution in the same lake, but a various distribution between different lakes [70]. The mean value of ^{238}U content in Keluke Lake ($5.5 \mu\text{g}/\text{L}$) was significantly lower than that in Tuosu Lake ($34.7 \mu\text{g}/\text{L}$) [70], implying a consistent and steady-state source of ^{230}Th in the same lake, with Tuosu Lake having a greater source. The sources of Th isotopes are very limited in the lake environment, among which the ^{232}Th isotope makes up approximately 99.98% of all natural Th isotopes, which are almost completely obtained by the dissolution of river, wind and lake sediments [29]. Thorium is particle reactive and, thus, easily eliminated from water by migration and removal of particles [71]. Therefore, the advection of the river and the content of particulate matter have a great impact on the content of ^{232}Th in lakes. Thorium isotope data showed large differences in thorium isotope content in different lakes, with Keluke Lake having much higher values than Tuosu Lake, which is the opposite to the uranium isotopes distribution in the lake water. The inputs from Bayin River to Keluke Lake may have been responsible for this phenomenon.

As the largest recharge river to Keluke Lake, Bayin River had greater mean values of ^{232}Th concentrations than the surface water of Keluke Lake and Tuosu Lake. The Th isotope data indicate that Bayin River carried a great amount of particulate matter when it recharged Keluke Lake, before mixing with the lake water and flowing into Tuosu Lake via the connecting river. The flux results indicate that Keluke Lake had much larger fluxes than Tuosu Lake in surface water and across the depth profiles due to the input from Bayin River (Figures 6 and 8a). The lower values of lithogenic flux in Tuosu Lake show that KLK–TS River contributed limited flux to this lake (Figure 8b). Therefore, in summer (June and July), the dust flux in this area could be estimated as $0.133 \text{ g}/\text{m}^2/\text{year}$, accounting for 8% of the total flux contribution to Keluke Lake.

In seawater, most of the dissolved ^{232}Th is produced by atmospheric dust that carries particulate matter and dissolves into the surface of seawater. Thus, the concentration of ^{232}Th in seawater decreases with depth and reaches a maximum at the sea surface [37,63,67]. Nevertheless, in both Tuosu Lake and Keluke Lake, the results in the depth profiles show that ^{232}Th concentration and lithogenic flux increased with depth (Figures 3 and 8b), which is highly consistent with the study of Zhang et al. [40]. Bayin River carried more exogenous detrital material into the lakes and mixed with the lake water, resulting in an increase in particle flux with depth.

According to the results of depth profiles in Keluke Lake and Tuosu Lake, the lithogenic fluxes delivered to the lake by rivers could be quantified to reflect the lithogenic fluxes on both seasonal and annual scales. In summer, the flux of lithogenic material from Bayin River to Keluke Lake was $12.367 \text{ g}/\text{m}^2/\text{year}$, calculated using the mean value of lithogenic fluxes at depth profiles in Keluke Lake. Meanwhile, the depth profile flux of Tuosu Lake could not be accurately calculated, due to the low concentration of ^{232}Th . Thus, unlike Keluke Lake, the main source of particle material flux in Tuosu Lake was atmospheric deposition,

and the contribution of the recharging river to the lake water flux was limited. There were significant seasonal variations of dissolved ^{232}Th and fluxes in both Keluke Lake and Tuosu Lake, showing a trend of high values in winter and low values in summer. In the alpine and arid regions, the flux of the two lakes in spring accounted for about 80% of the annual flux even in the freezing period.

There are two marine sources of Th: the first source is when the shallow layer is formed by the dissolution of dust, and the deep layer is formed by the dissolution/resuspension of sediment; the second source is a removal mechanism, the Th is scavenged by the water column [29]. Other explanations for the increasing trend of ^{232}Th concentration with depth in Tuosu and Keluke Lakes may be the redissolution of lake bottom sediments and the accumulated sinking flux [40]. In addition, the solubility of ^{232}Th in the particulate matter caused uncertainty when calculating the lithogenic fluxes. In the future, we will further explore the ^{232}Th isotope information of particulate material in the lake water and determine the solubility of ^{232}Th in particulate material, so as to more accurately evaluate the contribution of dust flux to the study area. Additionally, the Th composition and the size of dissolved and particulate material in the lake water and sediment will also be explored to quantify the ^{232}Th contribution to lake sediments.

When extending regional studies to the global ocean, the limnological conditions of the studied lakes are not exactly identical to those of the oceans. For the ocean, the source of particle flux includes not only detrital particulate matter, but also secondary products such as organic carbon, carbonate, and biogenic opal [72]. Due to the contribution of this fraction to ocean fluxes being variable, and due to the low partition coefficients between Th and both opal and organic carbon in seawater [71,72], there is variable solubility with several types of particulate matter. Therefore, the lithogenic flux evaluated by the ^{232}Th of the dissolved water could be more indicative of the source of detritus and/or dust. To accurately evaluate the deposition flux in the ocean, it is necessary to accurately evaluate the Th partition coefficients between seawater and several major types of particulate matter. For example, the flux evaluation of opal, organic carbon and carbonate based on the ^{232}Th of the dissolved water, needs to be further evaluated in the future. Furthermore, the lake fluxes in this study are basically consistent with the ocean results in terms of indicating limited dust input [73–75]. Thus, even though the conditions of the studied lakes and the open oceans are different, we believe that ^{232}Th can be used to assess lacustrine lithogenic flux in the studied region, with limited biological source contribution, which in turn could provide basic information for marine debris source flux.

5. Conclusions

There were significant differences in the concentration of ^{232}Th in the surface water of Tuosu Lake, but limited variation in Keluke Lake. The ^{232}Th concentrations and lithogenic flux in the horizontal spatial and vertical scales of Keluke Lake were significantly higher than those of Tuosu Lake in the same sampling season. The ^{232}Th concentration in the water of the study area was in the order Bayin River > Keluke Lake > KLK–TS River > Tuosu Lake, indicating that Bayin River carried a great amount of particulate matter when recharging Keluke Lake, before mixing with the lake water and flowing into Tuosu Lake via the connecting river. Furthermore, in both Tuosu Lake and Keluke Lake, the ^{232}Th concentration, dissolved ^{232}Th flux, and lithogenic flux were at least several times higher in winter than in summer, reaching their maximum values in February, which is consistent with the results observed in Qinghai Lake [40]. As a closed saltwater lake, the residence time of Tuosu Lake in December is 2–7 years, which is mainly affected by the sinking of particulate material. However, as an open freshwater lake, the residence time of Keluke Lake in June is less than 1 year, much lower than that of Tuosu Lake, which is mainly affected by the mixing of the young water from the recharge river with the lake.

In conclusion, there are three main influencing factors of lake lithofacies flux: the first is the contribution of the recharge river flow through channel with loose sediment, the second is the contribution of atmospheric dust, and the third is the influence of the

regional topography near the lake. On an interannual timescale, the lithogenic flux of Keluke Lake was mainly derived from river input. In June and July, the dust flux in the study area could be estimated as $0.133 \text{ g/m}^2/\text{year}$, while the flux of lithogenic material from Bayin River to Keluke Lake was $12.367 \text{ g/m}^2/\text{year}$. During the windy winter and spring, the deposition of atmospheric dust contributed a large amount of lithogenic flux to the lakes, and the regional topography of the two lakes resulted in a 36% lower flux in Tuosu Lake than in Keluke Lake. In addition to atmospheric deposition contributing a certain amount of dust flux to the lakes in the study area, Bayin River carried a large amount of debris into Keluke Lake. In contrast, the contribution of recharge rivers to Tuosu Lake was limited; the main source of lithogenic flux in the lake was dust flux, and the high values of ^{232}Th concentration and the lithogenic flux of depth profiles in the lake may have been caused by the resuspension of bottom sediments and the accumulation of sediment flux. This study confirms that the thorium series isotopes can be used as utility indicators of geological processes, namely, weathering and transport and/or atmospheric deposition. Additionally, an interpretation of lacustrine lithogenic flux based on dissolved ^{232}Th could further provide basic information for marine debris source flux.

Author Contributions: The research was supervised by P.Z. and X.L. with guidance provided by R.L.E. Samples were collected by P.Z., X.P., C.C. (Chi Chen), L.L., J.C., T.C. and X.L. The experiment method was instructed by P.Z. and C.C. (Chenyang Cao). The paper was written by C.C. (Chenyang Cao) and C.C. (Chi Chen) with revisions provided by P.Z., X.L. and R.L.E. All authors have read and agreed to the published version of the manuscript.

Funding: This study was supported by the National Natural Science Foundation of China (No. 41873013; No. 41888101), the Scientific Research Start-up Funds of Xi'an Jiaotong University (No. xxj032019007) and U.S. NSF (No. 1702816).

Data Availability Statement: The original contributions presented in the study are included in the article, and further inquiries can be directed to the corresponding authors.

Acknowledgments: We are grateful to the reviewers and editors for constructive comments on improvements to the quality and framework of the manuscript.

Conflicts of Interest: The authors declare no conflict of interest.

References

1. Rea, D.K. The paleoclimatic record provided by eolian deposition in the deep sea: The geologic history of wind. *Rev. Geophys.* **1994**, *32*, 159–195. [[CrossRef](#)]
2. Martin, J.H.; Gordon, R.M. Northeast Pacific iron distributions in relation to phytoplankton productivity. *Deep-Sea Res.* **1988**, *35*, 177–196. [[CrossRef](#)]
3. Jickells, T.D.; An, Z.S.; Andersen, K.K.; Baker, A.R.; Bergametti, G.; Brooks, N.; Cao, J.J.; Boyd, P.W.; Duce, R.A.; Hunter, K.A.; et al. Global iron connections between desert dust, ocean biogeochemistry, and climate. *Science* **2005**, *308*, 67–71. [[CrossRef](#)]
4. Martin, J.H.; Fitzwater, S.E. Iron deficiency limits phytoplankton growth in the north-east Pacific subarctic. *Nature* **1988**, *331*, 341–343. [[CrossRef](#)]
5. Duce, R.A.; Tindale, N.W. Atmospheric transport of iron and its deposition in the ocean. *Limnol. Oceanogr.* **1991**, *36*, 1715–1726. [[CrossRef](#)]
6. Martin, J.H. Glacial-interglacial CO_2 change: The Iron Hypothesis. *Paleoceanography* **1990**, *5*, 1–13. [[CrossRef](#)]
7. Cruz, J.A.; McDermott, F.; Turrero, M.J.; Edwards, R.L.; Martin-Chivelet, J. Strong links between Saharan dust fluxes, monsoon strength, and North Atlantic climate during the last 5000 years. *Sci. Adv.* **2021**, *7*, eabe6102. [[CrossRef](#)]
8. Mahowald, N.M.; Baker, A.R.; Bergametti, G.; Brooks, N.; Duce, R.A.; Jickells, T.D.; Kubilay, N.; Prospero, J.M.; Tegen, I. Atmospheric global dust cycle and iron inputs to the ocean. *Glob. Biogeochem. Cycles* **2005**, *19*, 1–15. [[CrossRef](#)]
9. Measures, C.I.; Brown, E.T. Estimating dust input to the Atlantic Ocean using surface water Aluminium Concentrations. In *The Impact of Desert Dust across the Mediterranean*; Springer: Dordrecht, The Netherlands, 1996.
10. Hsieh, Y.T.; Henderson, G.M.; Thomas, A.L. Combining seawater ^{232}Th and ^{230}Th concentrations to determine dust fluxes to the surface ocean. *Earth Planet. Sci. Lett.* **2011**, *312*, 280–290. [[CrossRef](#)]
11. Ojovan, M.I.; Lee, W.E. Naturally Occurring Radionuclides. In *An Introduction to Nuclear Waste Immobilisation*; Ojovan, M.I., Lee, W.E., Eds.; Elsevier: Oxford, UK, 2014; pp. 31–39.
12. Pérez-Tribouillier, H.; Noble, T.L.; Townsend, A.T.; Bowie, A.R.; Chase, Z. Quantifying lithogenic inputs to the southern ocean using long-lived Thorium isotopes. *Front. Mar. Sci.* **2020**, *7*, 207. [[CrossRef](#)]

13. Bacon, M.P.; van der Loeff, M.M.R. Removal of thorium-234 by scavenging in the bottom nepheloid layer of the ocean. *Earth Planet. Sci. Lett.* **1989**, *92*, 157–164. [[CrossRef](#)]
14. Clegg, S.L.; Whitfield, M. A generalized model for the scavenging of trace metals in the open ocean—I. Particle cycling. *Deep Sea Res.* **1990**, *37*, 809–832. [[CrossRef](#)]
15. Clegg, S.L.; Whitfield, M. A generalized model for the scavenging of trace metals in the open ocean—II. Thorium scavenging. *Deep Sea Res.* **1991**, *38*, 91–120. [[CrossRef](#)]
16. Dunne, J.P.; Murray, J.W.; Young, J.; Balistreri, L.S.; Bishop, J. ^{234}Th and particle cycling in the central equatorial Pacific. *Deep Sea Res. Part II* **1997**, *44*, 2049–2083. [[CrossRef](#)]
17. Murray, J.W.; Downs, J.N.; Strom, S.; Wei, C.L.; Jannasch, H.W. Nutrient assimilation, export production and ^{234}Th scavenging in the eastern equatorial Pacific. *Deep Sea Res.* **1989**, *36*, 1471–1489. [[CrossRef](#)]
18. Buesseler, K.O. The decoupling of production and particle export in the surface ocean. *Glob. Biogeochem. Cycles* **1998**, *12*, 297–310. [[CrossRef](#)]
19. Benitez-Nelson, C.; Buesseler, K.O.; Karl, D.M.; Andrews, J. A time-series study of particulate matter export in the North Pacific Subtropical Gyre based on ^{234}Th : ^{238}U disequilibrium. *Deep Sea Res.* **2001**, *48*, 2595–2611. [[CrossRef](#)]
20. Moore, W.S. The thorium isotope content of ocean water. *Earth Planet. Sci. Lett.* **1981**, *53*, 419–426. [[CrossRef](#)]
21. Anderson, R.F.; Fleisher, M.Q.; Biscaye, P.E.; Kumar, N.; Dittrich, B.; Kubik, P.; Suter, M. Anomalous boundary scavenging in the Middle Atlantic Bight: Evidence from ^{230}Th , ^{231}Pa , ^{10}Be and ^{210}Pb . *Deep Sea Res.* **1994**, *41*, 537–561. [[CrossRef](#)]
22. Santschi, P.H.; Guo, L.; Walsh, I.D.; Quigley, M.S.; Baskaran, M. Boundary exchange and scavenging of radionuclides in continental margin waters of the Middle Atlantic Bight: Implications for organic carbon fluxes. *Cont. Shelf Res.* **1999**, *19*, 609–636. [[CrossRef](#)]
23. Smoak, J.M.; Moore, W.S.; Thunell, R.C. Influence of boundary scavenging and sediment focusing on ^{234}Th , ^{228}Th and ^{210}Pb fluxes in the Santa Barbara Basin. *Estuar. Coast. Shelf Sci.* **2000**, *51*, 373–384. [[CrossRef](#)]
24. Yu, E.F.; Francois, R.; Bacon, M.P. Similar rates of modern and last-glacial ocean thermohaline circulation inferred from radiochemical data. *Nature* **1996**, *379*, 689–694. [[CrossRef](#)]
25. Marchal, O.; François, R.; Stocker, T.F.; Joos, F. Ocean thermohaline circulation and sedimentary $^{231}\text{Pa}/^{230}\text{Th}$ ratio. *Paleoceanography* **2000**, *15*, 625–641. [[CrossRef](#)]
26. Moran, S.B.; Shen, C.C.; Edmonds, H.N.; Weinstein, S.E.; Smith, J.N.; Edwards, R.L. Dissolved and particulate ^{231}Pa and ^{230}Th in the Atlantic Ocean: Constraints on intermediate/deep water age, boundary scavenging, and $^{231}\text{Pa}/^{230}\text{Th}$ fractionation. *Earth Planet. Sci. Lett.* **2002**, *203*, 999–1014. [[CrossRef](#)]
27. Santschi, P.H.; Murray, J.W.; Baskaran, M.; Benitez-Nelson, C.R.; Guo, L.D.; Hung, C.C.; Lamborg, C.; Moran, S.B.; Passow, U.; Roy-Barman, M. Thorium speciation in seawater. *Mar. Chem.* **2006**, *100*, 250–268. [[CrossRef](#)]
28. Bourdon, B.; Turner, S.; Dosseto, A. Dehydration and partial melting in subduction zones: Constraints from U-series disequilibria. *J. Geophys. Res.* **2003**, *108*, 2291. [[CrossRef](#)]
29. Krishnaswami, S.; Cochran, J.K. Uranium-Thorium series radionuclides in ocean profiles. *Encycl. Ocean Sci.* **2016**, *1*, 377–391.
30. Krishnaswami, S.; Cochran, J.K. *Radioactivity in the Environment*; Elsevier: Amsterdam, The Netherlands, 2008.
31. Zhang, P.; Cheng, H.; Liu, W.G.; Mo, L.T.; Li, X.Z.; Ning, Y.F.; Ji, M.; Zong, B.Y.; Zhao, C. Geochemical and isotopic (U, Th) variations in lake waters in the Qinghai Lake Basin, Northeast Qinghai-Tibet Plateau, China: Origin and paleoenvironmental implications. *Arab. J. Geosci.* **2019**, *12*, 92. [[CrossRef](#)]
32. Costa, K.; McManus, J. Efficacy of ^{230}Th normalization in sediments from the Juan de Fuca Ridge, northeast Pacific Ocean. *Geochim. Cosmochim. Acta* **2017**, *197*, 215–225. [[CrossRef](#)]
33. Broecker, W.S.; Kaufman, A.; Trier, R.M. The residence time of thorium in surface sea water and its implications regarding the rate of reactive pollutants. *Earth Planet. Sci. Lett.* **1973**, *20*, 35–44. [[CrossRef](#)]
34. Scholten, J.C.; Loeff, M.; Michel, A. Distribution of ^{230}Th and ^{231}Pa in the water column in relation to the ventilation of the deep Arctic basins. *Deep Sea Res. Part II Top. Stud. Oceanogr.* **1995**, *42*, 1519–1531. [[CrossRef](#)]
35. Chase, Z.; Anderson, R.F.; Fleisher, M.Q.; Kubik, P.W. Scavenging of ^{230}Th , ^{231}Pa and ^{10}Be in the Southern Ocean (SW Pacific sector): The importance of particle flux, particle composition and advection. *Deep Sea Res. Part II Top. Stud. Oceanogr.* **2003**, *50*, 739–768. [[CrossRef](#)]
36. Hayes, C.T.; Anderson, R.F.; Fleisher, M.Q.; Serno, S.; Winckler, G.; Gersonde, R. Quantifying lithogenic inputs to the North Pacific Ocean using the long-lived thorium isotopes. *Earth Planet. Sci. Lett.* **2013**, *383*, 16–25. [[CrossRef](#)]
37. Hayes, C.T.; Rosen, J.; Mcgee, D.; Boyle, E.A. Thorium distributions in high- and low-dust regions and the significance for iron supply. *Glob. Biogeochem. Cycles* **2017**, *31*, 328–347. [[CrossRef](#)]
38. Hayes, C.T.; Fitzsimmons, J.N.; Boyle, E.A.; McGee, D.; Anderson, R.F.; Weisend, R.; Morton, P.L. Thorium isotopes tracing the iron cycle at the Hawaii Ocean Time-series Station ALOHA. *Geochim. Cosmochim. Acta* **2015**, *169*, 1–16. [[CrossRef](#)]
39. Deng, F.F.; Thomas, A.L.; Rijkenberg, M.J.A.; Henderson, G.M. Controls on seawater ^{231}Pa , ^{230}Th and ^{232}Th concentrations along the flow paths of deep waters in the Southwest Atlantic. *Earth Planet. Sci. Lett.* **2014**, *390*, 93–102. [[CrossRef](#)]
40. Zhang, P.; Pei, X.Z.; Cao, C.Y.; Chen, C.; Gong, Z.Q.; Li, X.R.; Pang, J.Y.; Liang, L.H.; Li, X.Z.; Ning, Y.F.; et al. A novel tracer technique to quantify the lithogenic input flux of trace elements to Qinghai Lake. *Front. Earth Sci.* **2022**, *10*, 866314. [[CrossRef](#)]
41. Zhao, Y.; Yu, Z.; Liu, X.; Zhao, C.; Chen, F.; Zhang, K. Late Holocene vegetation and climate oscillations in the Qaidam Basin of the northeastern Tibetan Plateau. *Quat. Res.* **2010**, *73*, 59–69. [[CrossRef](#)]

42. Lister, G.S.; Kelts, K.; Chen, K.Z.; Yu, J.Q.; Niessen, F. Lake Qinghai, China: Closed-basin like levels and the oxygen isotope record for ostracoda since the latest Pleistocene. *Palaeogeogr. Palaeoclimatol. Palaeoecol.* **1991**, *84*, 141–162. [[CrossRef](#)]
43. Henderson, A.; Holmes, J.A. Palaeolimnological evidence for environmental change over the past millennium from Lake Qinghai sediments: A review and future research prospective. *Quat. Int.* **2009**, *194*, 134–147. [[CrossRef](#)]
44. Zhao, Y.; Yu, Z.; Chen, F.; Liu, X.; Ito, E. Sensitive response of desert vegetation to moisture change based on a near-annual resolution pollen record from Gahai Lake in the Qaidam Basin, northwest China. *Glob. Planet. Chang.* **2008**, *62*, 107–114. [[CrossRef](#)]
45. Dietze, E.; Wünnemann, B.; Hartmann, K.; Diekmann, B.; Jin, H.; Stauch, G.; Yang, S.; Lehmkuhl, F. Early to mid-Holocene lake high-stand sediments at Lake Donggi Cona, northeastern Tibetan Plateau, China. *Quat. Res.* **2013**, *79*, 325–336. [[CrossRef](#)]
46. Rao, Z.; Jia, G.; Qiang, M.; Zhao, Y. Assessment of the difference between mid- and long chain compound specific δD_n -alkanes values in lacustrine sediments as a paleoclimatic indicator. *Org. Geochem.* **2014**, *76*, 104–117. [[CrossRef](#)]
47. Wang, S.P.; Jia, G.D.; Zhao, Y.; Rao, Z.G. Plant wax n-alkanes record of the Holocene paleoclimatic changes from a core sediment of Hurlig lake in the Qaidam Basin. *Quat. Sci.* **2010**, *30*, 1098–1104. (In Chinese)
48. Zhao, Y.; Yu, Z.; Chen, F.; Ito, E.; Zhao, C. Holocene vegetation and climate history at Hurlig Lake in the Qaidam Basin, northwest China. *Rev. Palaeobot. Palynol.* **2007**, *145*, 275–288. [[CrossRef](#)]
49. Chen, Z.Y.; Dong, Z.B.; Wang, Q.C.; Chong, Y.E.; Liu, F. Characteristics of wind regime and sand drift potential in Qaidam Basin of China. *J. Desert Res.* **2020**, *40*, 195–203. (In Chinese)
50. Bao, F.; Dong, Z.B.; Zhang, Z.C. Wind regime in the Qaidam Basin desert. *J. Desert Res.* **2015**, *35*, 549–554. (In Chinese)
51. Wang, Y.H.; Liu, Y.X.; Liu, H.H.; Liu, X.L.; Lu, Z.K.; Li, J. Chemical composition and heavy metal distribution in surface water of typical inland rivers in Qinghai. *Chin. J. Ecol.* **2018**, *37*, 734–742. (In Chinese)
52. Yi, X.; Yang, D.; Xu, W. *China Regional Hydrogeology Survey Report—Toson Lake Map (J-47-[25] 1:200,000)*; Qaidam Integrative Geology Survey: Golmud, Qinghai, China, 1992. (In Chinese)
53. Zhao, C.; Yu, Z.; Zhao, Y.; Ito, E. Possible orographic and solar controls of Late Holocene centennial-scale moisture oscillations in the northeastern Tibetan Plateau. *Geophys. Res. Lett.* **2009**, *36*, 1–6. [[CrossRef](#)]
54. Long, Q.F.; Feng, X.Y.; Liu, J.; Zhang, X.; Shen, G.P.; Zhu, D.R. Microbial diversity of Keluke-Tuosu Lake wetland reserve in Qinghai-Tibet Plateau. *Earth Environ.* **2017**, *45*, 399–407. (In Chinese)
55. Wang, S.M.; Dou, H.S. *Lakes in China*; Science Press: Beijing, China, 1998. (In Chinese)
56. Fu, X.; Zhang, J.W.; Wang, L.; Cui, X.L.; Ma, X.Y.; Zhang, Y.Z. Recent human impacts on sedimentary record: A case from Lake Toson. *Quat. Sci.* **2016**, *36*, 1456–1465. (In Chinese)
57. Cheng, H.; Edwards, R.L.; Hoff, J.; Gallup, C.D.; Richards, D.A.; Asmerom, Y. The half-lives of uranium-234 and thorium-230. *Chem. Geol.* **2000**, *169*, 17–33. [[CrossRef](#)]
58. Cheng, H.; Edwards, R.L.; Shen, C.C.; Polyak, V.J.; Asmerom, Y.; Woodhead, J.; Hellstrom, J.; Wang, Y.J.; Kong, X.G.; Spötl, C.; et al. Improvements in ^{230}Th dating, ^{230}Th and ^{234}U half-life values, and U–Th isotopic measurements by multi-collector inductively coupled plasma mass spectrometry. *Earth Planet. Sci. Lett.* **2013**, *371–372*, 82–91. [[CrossRef](#)]
59. Shen, C.C.; Edwards, R.L.; Cheng, H.; Dorale, J.A.; Thomas, R.B.; Moran, S.B.; Weinstein, S.E.; Edmonds, H.N. Uranium and thorium isotopic and concentration measurements by magnetic sector inductively coupled plasma mass spectrometry. *Chem. Geol.* **2002**, *185*, 165–178. [[CrossRef](#)]
60. Shen, C.C.; Wu, C.C.; Cheng, H.; Edwards, R.L.; Hsieh, Y.T.; Gallet, S.; Chang, C.C.; Li, T.Y.; Lam, D.D.; Kano, A.; et al. High-precision and high-resolution carbonate ^{230}Th dating by MC-ICP-MS with SEM protocols. *Geochim. Cosmochim. Acta* **2012**, *99*, 71–86. [[CrossRef](#)]
61. Roy-Barman, M.; Lemaître, C.; Ayrault, S.; Jeandel, C.; Souhaut, M.; Miquel, J.C. The influence of particle composition on Thorium scavenging in the Mediterranean Sea. *Earth Planet. Sci. Lett.* **2009**, *286*, 526–534. [[CrossRef](#)]
62. Ankney, M.; Bacon, C.; Valley, J.; Beard, B.; Johnson, C. Oxygen and U–Th isotopes and the timescales of hydrothermal exchange and melting in granitoid wall rocks at Mount Mazama, Crater Lake, Oregon. *Geochim. Cosmochim. Acta* **2017**, *213*, 137–154. [[CrossRef](#)]
63. Edmonds, H.N.; Moran, S.B.; Hai, C.; Edwards, R.L. ^{230}Th and ^{231}Pa in the Arctic Ocean: Implications for particle fluxes and basin-scale Th/Pa fractionation. *Earth Planet. Sci. Lett.* **2004**, *227*, 155–167. [[CrossRef](#)]
64. Hayes, C.T.; Black, E.E.; Anderson, R.F.; Baskaran, M.; Buesseler, K.O.; Charette, M.A.; Cheng, H.; Cochran, J.K.; Edwards, R.L.; Fitzgerald, P.; et al. Flux of particulate elements in the North Atlantic Ocean constrained by multiple radionuclides. *Glob. Biogeochem. Cycles* **2018**, *32*, 1738–1758. [[CrossRef](#)]
65. Wang, X.Q.; Zhou, J.; Xu, S.F.; Chi, Q.H.; Nie, L.S.; Zhang, B.M.; Yao, W.S.; Wang, W.; Liu, H.L.; Liu, D.S.; et al. China soil geochemical baselines networks: Data characteristics. *Geol. China* **2016**, *43*, 12. (In Chinese)
66. Cochran, J.K.; Hirschberg, D.J.; Livingston, H.D.; Buesseler, K.O.; Robert, M.K. Natural and anthropogenic radionuclide distributions in the Nansen Basin, Arctic ocean: Scavenging rates and circulation timescales. *Top. Stud. Oceanogr.* **1995**, *42*, 1495–1517. [[CrossRef](#)]
67. Edmonds, H.N.; Moran, S.B.; Hoff, J.A.; Smith, J.N.; Edwards, R.L. Protactinium-231 and thorium-230 abundances and high scavenging rates in the western arctic ocean. *Science* **1998**, *280*, 405–407. [[CrossRef](#)] [[PubMed](#)]
68. Huh, C.A.; Bacon, M.P. Thorium-232 in the eastern Caribbean Sea. *Nature* **1985**, *316*, 718–721. [[CrossRef](#)]
69. Moore, W.S.; Sackett, W.M. Uranium and thorium series inequilibrium in sea water. *J. Geophys. Res.* **1964**, *69*, 5401–5405. [[CrossRef](#)]

70. Zhao, C.; Zhang, P.; Li, X.Z.; Ning, Y.F.; Tan, L.C.; Edwards, R.L.; Yao, X.N.; Cheng, H. Distribution characteristics and influencing factors of uranium isotopes in saline lake waters in the northeast of Qaidam Basin. *Minerals* **2020**, *10*, 74. [[CrossRef](#)]
71. Kretschmer, S.; Geibert, W.; Loeff, M.; Mollenhauer, G. Grain size effects on ^{230}Th s inventories in opal-rich and carbonate-rich marine sediments. *Earth Planet. Sci. Lett.* **2010**, *294*, 131–142. [[CrossRef](#)]
72. Chase, Z.; Anderson, R.F.; Fleisher, M.Q.; Kubik, P. The influence of particle composition and particle flux on scavenging of Th, Pa and Be in the ocean. *Earth Planet. Sci. Lett.* **2002**, *204*, 215–229. [[CrossRef](#)]
73. Honjo, S.; Francois, R.; Manganini, S.; Dymond, J.; Collier, R. Particle fluxes to the interior of the Southern Ocean in the Western Pacific sector along 170-degree W. *Deep Sea Res. II* **2000**, *47*, 3521–3548. [[CrossRef](#)]
74. Measures, C.I.; Vink, S. On the use of dissolved aluminum in surface waters to estimate dust deposition to the ocean. *Glob. Biogeochem. Cycles* **2000**, *14*, 317–327. [[CrossRef](#)]
75. Chase, Z.; Anderson, R.F.; Fleisher, M.Q.; Kubik, P.W. Accumulation of biogenic and lithogenic material in the Pacific sector of the Southern Ocean during the past 40,000 years. *Deep Sea Res. Part II* **2003**, *50*, 799–832. [[CrossRef](#)]